ELSEVIER

Polymer 41 (2000) 6171–6180

polymer

Observations of water migration during thermoporometry studies of cellulose films

J.N. Hay*, P.R. Laity

School of Metallurgy and Materials, University of Birmingham, Edgbaston, Birmingham B15 2TT, UK

Received 29 June 1999; received in revised form 25 October 1999; accepted 5 November 1999

Abstract

Thermoporometry is widely used for measuring pore size distribution in porous materials by differential scanning calorimetry based on melting point depression and the Gibbs–Thomson effect shown by a liquid contained in the pores. However, measurements on water-swollen cellophane showed that the shapes of heat flow vs. temperature plots (and, therefore, derived pore size distributions) changed with heating rate. Results obtained in heating were the product of two sequential and overlapping effects: an endothermic melting of the smallest ice crystals within pores in the film, followed by diffusion of the water and an exothermic re-freezing on larger crystals at the film surface. This caused the volume of larger pores to be underestimated or missed completely. In contrast, diffusion out of the smallest pores preceded freezing for measurements on cooling, so only the larger pores were observable.

The rate of diffusion was estimated as 1×10^{-13} m^2 s^{-1} from the quantities of ice in pores and at the film surface observed at different heating rates. The value obtained was much slower than expected for water-swollen cellulose, but consistent with water diffusion through dry cellulose, suggesting that the film surface had been 'freeze-dried' during the measurements.

Keywords: Water migration; Thermoporometry; Cellulose films

1. Introduction

Thermoporometry is a method for measuring pore size distribution, based on the depression of melting temperature of materials constrained within small pores [1]. Measurements are relatively easily made by differential scanning calorimetry (DSC) and can be performed on fragile samples containing pores of 2–50 nm radius, which cannot be readily studied by other methods [2]. It is particularly well suited for studying swollen samples. Thermoporometry has, therefore, become a popular tool for measuring pore size distribution in polymer membranes —as illustrated in reviews by Nakao [3] and Kim et al. [4] and numerous publications by other authors [5–12].

2. Development of thermoporometry

The depression of melting temperature experienced by substances constrained in small pores is well known. In 1920 Tammann described an apparatus for studying melting point depressions for thin films of materials [13]. Using this apparatus, Meissner observed small depressions of melting temperature for crystals about 0.8 μm thick [14].

In 1932 Kubelka [15] reported that iodine absorbed into porous carbon remained liquid at room temperature (normal melting point for 'bulk' iodine is 386.6 K) and proposed an explanation based on the effect of surface energy on the stability of small crystals. The effect of surface energy on melting temperature (known as the Gibbs–Thomson effect) has been discussed in detail by Reiss and Wilson [16], Still and Skapski [17] and Woodruff [18]. Skapski successfully applied the theory to the formation of ice crystals in clouds at different degrees of undercooling [19].

The first suggestions that melting temperature depression could be used to study pore sizes were made by Kuhn et al. in 1955. These authors demonstrated melting temperature depression of about 2 K for water in poly(vinyl aclohol)–poly(acrylic acid) gels [20] and 5 K for benzene absorbed in lightly cross-linked rubber [21]. They also observed the migration of solvent between freezing experiments. However, their rather limited apparatus prevented quantitative measurements.

A detailed theoretical basis for thermoporometry was established by Brun et al. in 1977 [1]. Starting from an application of the Gibbs–Duhem equation to the solid, liquid and vapour interfaces and making some reasonable

* Corresponding author. Tel.: +44-121-414-4544; fax: +44-121-414-5232.

0032-3861/00/$ - see front matter
PII: S0032-3861(99)00828-9

Table 1
Numerical values for constants in Eqs. (1) and (3) (after Brun et al. [1])

	A (nm)	B (nm K)	C (J g^{-1} K^{-1})	D (J g^{-1} K^{-2})
Water, heating in cylindrical pores	0.68	32.33	11.39	0.155
Water, cooling or spherical pores	0.57	64.67	7.43	0.0556
Benzene, heating in cylindrical pores	0.92	65.8	2.94	0.0273
Benzene, cooling or spherical pores	0.54	131.6	1.76	0.00887

assumptions concerning bound layers of liquid which did not undergo phase changes, they established that the pore radius (R_p) and differential pore volume (dV/dR_p) could be calculated from the melting point depression (ΔT, which is negative for lowered melting temperature) and heat flow (dq/dt). The equations derived by Brun et al. [1] were:

$$R_p = A - \frac{B}{\Delta T} \quad (1)$$

$$\frac{dV}{dR_p} = \frac{k(\Delta T^2)(dq/dt)}{\Delta H_a(T)} \quad (2)$$

where k is a 'calibration constant' accounting for the instrument sensitivity, sample mass and heating rate. The apparent heat of fusion, $\Delta H_a(T)$, was temperature dependent:

$$\Delta H_a(T) = \Delta H_f + C\Delta T + D(\Delta T)^2 \quad (3)$$

where ΔH_f is the heat of fusion for the penetrant liquid under normal conditions (332 J g^{-1} for water). The numerical values of the constants A to D depended on whether the measurements were made in heating or cooling, pore geometry and penetrant liquid. The values obtained by Brun et al. for water and benzene, for R_p expressed in nanometres and ΔH_a in J g^{-1}, are shown in Table 1. The validity of their model was checked by comparing thermoporometry measurements with pore sizes determined by the nitrogen adsorption–desorption method devised by Barrett et al. [22].

For the present study, water was used as the penetrating liquid, since the characteristics of the swollen membranes in an aqueous environment was of interest to us. Pore radius was calculated on the assumption of cylindrical pore shape. This is unlikely to be absolutely correct, but is believed to be a reasonable approximation for the elongated voids expected within the cellophane films used in this study. It is also consistent with assumptions of pore shape made by other workers using thermoporometry [3–6,9–11] and other techniques [23,24] to study porosity in regenerated cellulose and other polymer membranes. Indeed, by comparing melting and freezing heat flow vs. temperature curves, Quinson et al. [12] confirmed the validity of the cylindrical pore model for a polycarbonate membrane.

3. Interactions of water with cellulose

The effects of moisture on cellulose are quite dramatic,

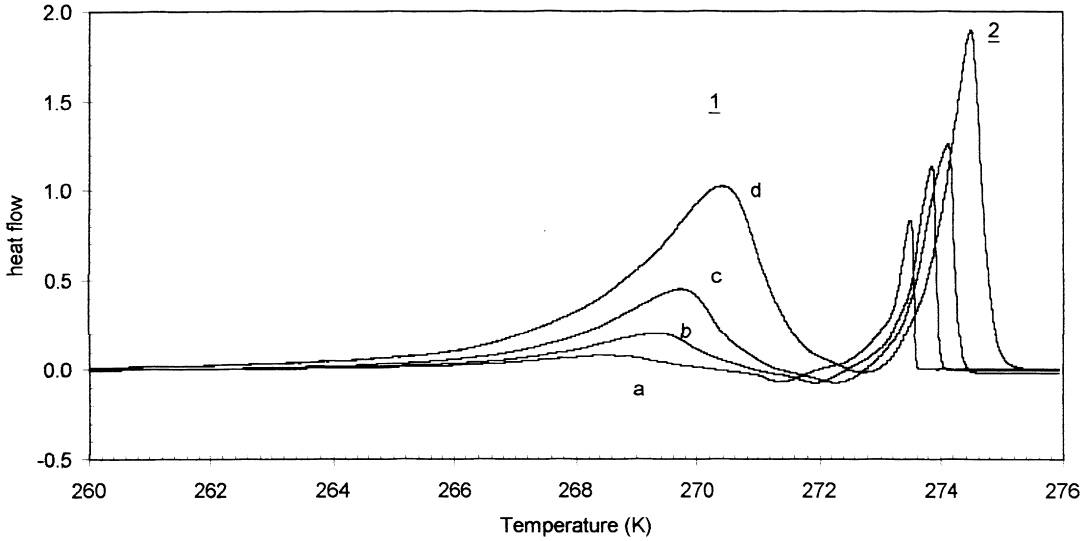

Fig. 1. Heat flow vs. temperature plots for wet cellophane at different heating rates: pore water (peak 1); bulk water (peak 2). Heating rates: 0.62 K min^{-1} (curve a); 1.25 K min^{-1} (curve b); 2.5 K min^{-1} (curve c); 5.0 K min^{-1} (curve d).

Table 2
Description of sample used in water migration measurements

Sample weight (mg)	1.71
Weight of cellulose (mg)	0.57
Weight of water (gravimetric) (mg)	1.14
(DSC) (mg)	0.81
Sample diameter (mm)	5
Sample thickness (μm)	65

causing extensive swelling with corresponding changes in mechanical properties. For example, it is well known that regenerated cellulose fibres (e.g. rayon and lyocell) have lower strength and modulus in the wet state compared with the 'conditioned state' of ambient moisture levels (typically about 10% water by weight). The plasticising effect of water in regenerated cellulose has been demonstrated by Stratton [25] and by Bradley and Carr [26], using dynamic mechanical analysis (DMA), and by Baum [27] and Hongo et al. [28] using thermally stimulated depolarisation current (TSDC) analysis. A comprehensive study of structural and mechanical changes due to moisture in cellophane has been reported by Yano and Hatakeyama [29]. Most of the absorbed water is assumed to be held within pores or amorphous regions of the cellulose; however, Yano and Hatakeyama [29] and other authors [30–32] have presented evidence that water was also able to diffuse into cellulose II crystals (the crystalline form usually present in regenerated cellulose) under some conditions.

DSC studies have played an important part in investigating the interactions between water and cellulose [33–45]. It has been found that water absorbed by cellulose can be classified into three distinct but interchangeable types:

1. 'Bulk' water was observed with a melting point at 273.15 K. This was interpreted as water outside the cellulose structure, so the melting temperature was not affected by interaction with the cellulose or the Gibbs–Thomson effect inside pores.
2. Some water was characterised by a melting temperature a few degrees below 273.15 K. Two explanations have been offered for this depression. Hatakeyama et al. [33–38] and others [39–43] suggested that the melting temperature depression was due to 'weak interaction' between water and cellulose chains. Taniguchi and Horigome [44] offered a similar interpretation for a low temperature melting peak for water in cellulose acetate. In contrast, Berghoff and Pusch [45] interpreted this as water held within pores, with the melting temperature being depressed by the Gibbs–Thomson effect. The latter interpretation has been assumed in the present work, for reasons, which are discussed below.
3. 'Non-freezing' water was identified as the difference between the total water (e.g. measured gravimetrically, by drying to constant weight) and water in the previous two categories, which was quantified from the heats of melting observed by DSC. Non-freezing water was generally assumed to be intimately hydrogen-bonded to cellulose chains. Hatakeyama et al. [36] reported about 0.4 g of this water per gram of cellulose in regenerated film, while Higuchi et al. [43] reported 1.06 g g^{-1}.

Higuchi et al. [43] also observed that the relative amounts of bulk and pore water indicated by the heat-flow vs. temperature plots depended on the heating rate used in the DSC experiment. This was ascribed to the re-freezing of water melted below 273.15 K, given sufficient time, and its subsequent re-melting along with bulk water. If bulk water existed outside the cellulose sample, while the pore water was contained within the cellulose, re-freezing would appear to involve migration of water from within the cellulose during the DSC experiment, along the lines proposed by Kuhn et al. [20,21].

Clearly, water migration and corresponding changes in shapes of heat-flow vs. temperature plots with DSC heating rate pose a serious problem to thermoporometry studies. The present work was carried out to investigate the scale of this problem. Water migration during the DSC experiment is also discussed in relation to the structure of cellophane and other studies of water diffusion through regenerated cellulose.

4. Experimental

DSC measurements were made using a Perkin–Elmer DSC-2 with a controlled cooling accessory to cool the block to 203 K. Pieces of regenerated cellulose film (uncoated cellophane manufactured by UCB Films Plc. Wigton) were washed in water, to remove plasticiser, and stored wet until required.

Wet film samples (1–5 mg, after removing surface water with a tissue) were sealed in tared aluminium DSC pans. The temperature was dropped rapidly to 230 K, then held for several minutes to freeze the water, as indicated by an exothermic peak. The samples were then heated (at a rate of 10 K min^{-1}) to the required starting temperature (250.0 or 272.0 K). Heat flow measurements were usually made while the samples were heated from 250.0 to 276.0 K against an empty pan as reference. For comparison, some measurements were also made as the samples were cooled from 272.0 to 250.0 K, following the method reported by Ishikiriyama et al. [6]. The instrumental baseline was checked using two similar empty pans; temperature and heat flow calibrations were checked with water.

After completing the DSC measurements, the sample pans were re-weighed (to check that water had not escaped during the experiment). The sample pans were punctured and then dried to constant weight in an oven at 393 K, to determine the total weight of water which had been contained in the sample.

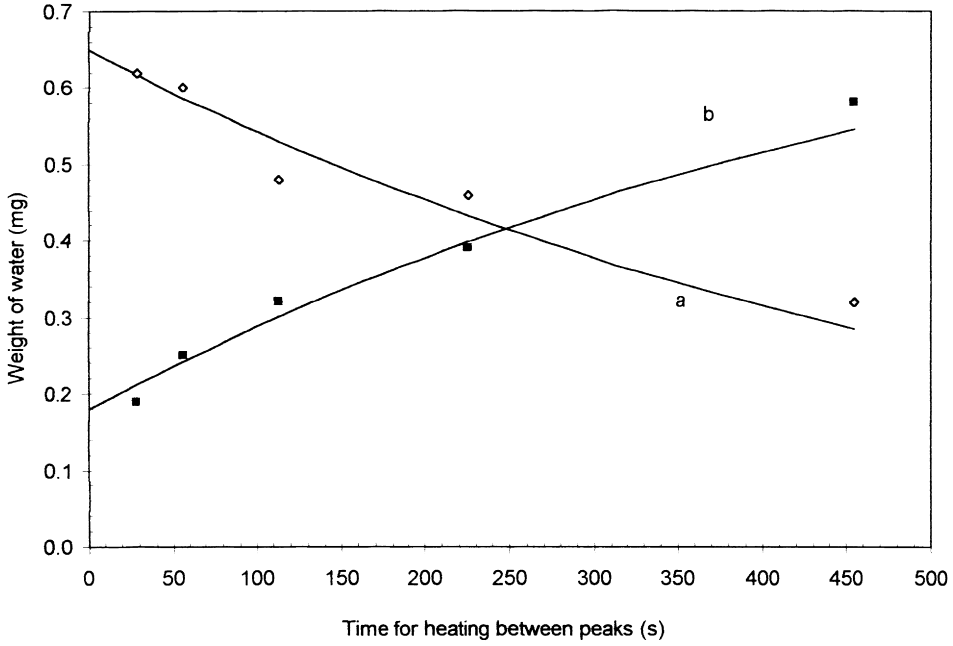

Fig. 2. Quantities of water melting observed in pores (curve a) and bulk (curve b) at different heating rates (for sample description, see Table 2).

5. Results

Below 260 K, the heat flow vs. temperature plots closely followed the instrumental baseline, which was essentially straight, horizontal and featureless. Above this temperature, two endotherms were observed, ascribed to water in pores (about 269–271 K) and bulk water (about 273–275 K). In order to compensate for thermal lag, measurements were made at several heating rates (0.62–5 K min^{-1}) and extrapolated to isothermal conditions. Typical results are shown in Fig. 1.

As well as shifting to higher temperature with faster heating rates (due to thermal lag in the instrument and sample), the heat flow vs. temperature plots changed shape. The area of the lower temperature melting endotherm (corresponding to water inside pores) increased in proportion from the slowest heating rate (0.62 K min^{-1}) to the fastest (5 K min^{-1}). A small negative peak was also observed (about 271–272 K) during some of the heating runs.

The amounts of water melting were quantified from the peak areas using Eq. (3) and plotted against the time taken to heat between the two peaks at different heating rates (Fig. 2). The total water apparently remained constant (0.81 ± 0.04 mg), while the proportion observed in the lower temperature peak increased and that in the bulk water decreased with heating rate.

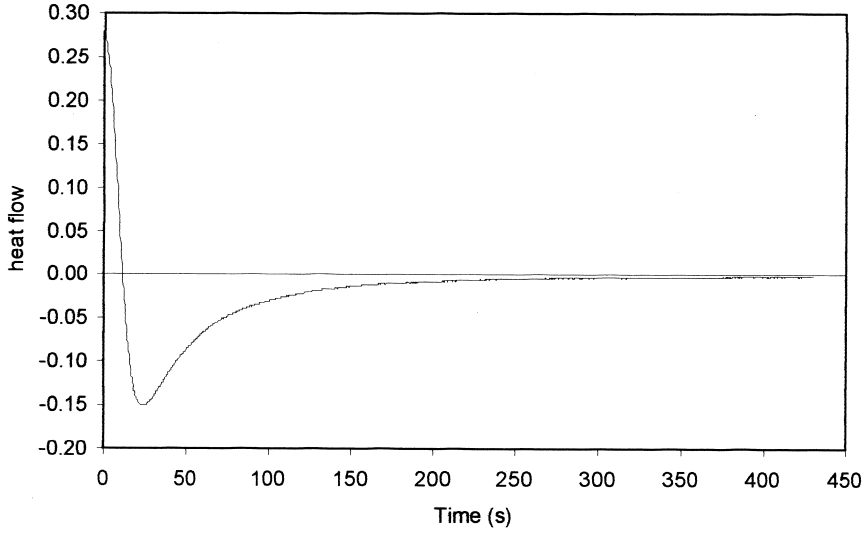

Fig. 3. Isothermal heat evolution (heating interrupted at 270.0 K).

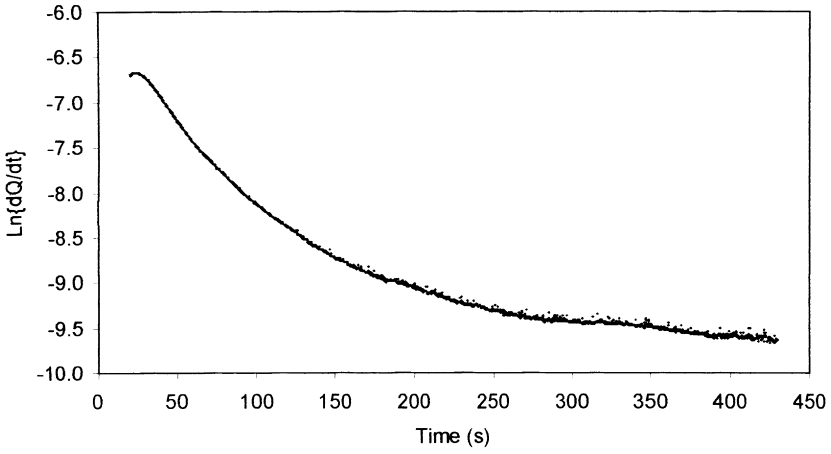

Fig. 4. Plot of ln{water recrystallisation rate} vs. time.

The balance between water melting in pores and bulk water suggested a migration from one melting domain to the other. The transfer from pore water to bulk water appeared to follow an exponential decay, which would be consistent with a diffusion process. The curves shown in Fig. 2 were obtained by manually fitting the following models, which are based on first order kinetics for the transfer of water out of pores and into the bulk, to the experimental data:

$$\text{Water in pores (in mg)}: \quad Q_{\text{pore}} = 0.65 \exp\{-t/550\} \tag{4a}$$

$$\text{Bulk water (in mg)}: \quad Q_{\text{bulk}} = 0.18 + 0.65 \times (1 - \exp\{-t/550\}) \tag{4b}$$

where t is the time in seconds to heat between the two peaks. The significance of these models will be discussed below.

Stopping the heating near the end of the lower peak (270.0 K) was followed by heat evolution, and a gradual return to the baseline over several minutes (Fig. 3). The first part of the curve with negative slope (up to about 25 s) represented the instrumental response; the second part, with positive slope, was interpreted as water migrating and re-freezing. The rate (dQ/dt) at which the water re-froze was determined from the heat flow and the apparent heat of fusion (taken as 310 J g^{-1} at 270.0 K, from Eq. (3). A plot of $\ln\{dQ/dt\}$ vs. time for the data from about 20 to 430 s is shown in Fig. 4. The results fell on a curve, indicating that a single exponential model was not sufficient, in this case. The isothermal temperature chosen (270.0 K) was equivalent to melting water in pores of radius less than approximately 11 nm; water in pores larger than this would have remained frozen. It is possible, therefore, that re-freezing could have occurred in a range of larger pores within the cellophane as well as at the film surface, which might explain why a more complex model appeared to be required in this case.

The migration of water out of the pores was confirmed by re-freezing and re-measuring the sample after partial melting. After interrupting the heating run at 270.0 K, the separate low temperature peak associated with water in pores was not observable in the re-measured sample (Fig. 5), although a small amount of water with slightly depressed

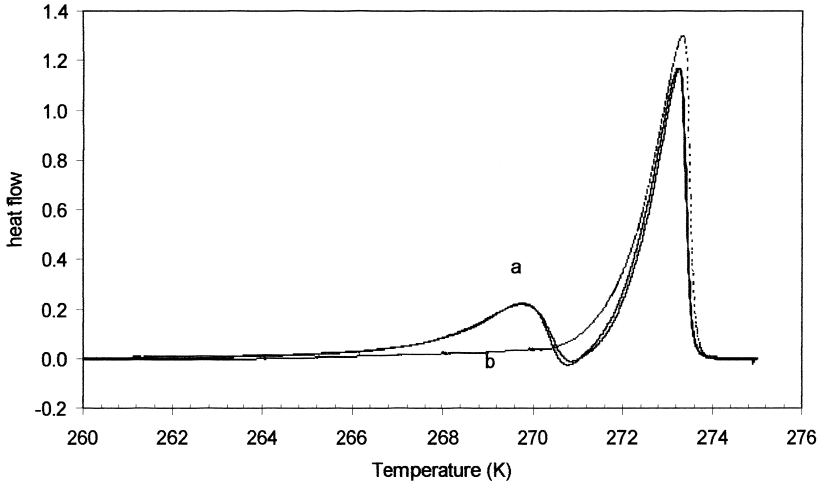

Fig. 5. Effect of interrupted heating on pore water peak: (a) represents first and last melting curves; and (b) represents after heating interrupted at 270.0 K.

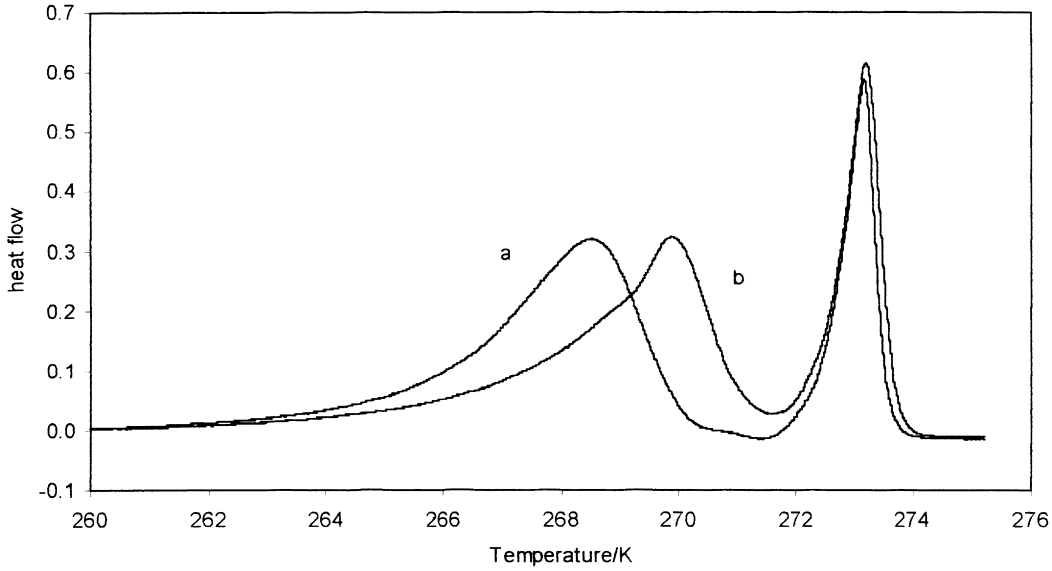

Fig. 6. Effect of interrupted heating on pore water peak: (a) represents first melting curve; and (b) represents after heating interrupted at 267.5 K.

melting temperature (equivalent to ice in larger pores) appeared as a low temperature tail on the peak associated with bulk water. The bulk water peak increased slightly in area, so that the total quantity of water melting again remained constant.

The lower temperature peak reappeared after completely melting, re-freezing and re-measuring the sample within a few minutes, so that the 'first' and 'last' traces were almost identical. Clearly, the return of water into the pores was also a fairly quick process, at least with the cellophane studied here, although no attempt was made to measure the rate.

The similarity between 'first' and 'last' traces indicated that the pore size distribution in the cellophane was not changed between repeated measurements, suggesting that the pores were not damaged by the volume increase associated with water freezing. Several possible explanations for this may be suggested. Cellophane is actually manufactured in a highly water-swollen state, which collapses on drying. The resulting film is reasonably elastic, with its thickness increasing more than twofold during free swelling with water from 'dry' to 'saturated' conditions. So the volume increase associated with ice formation may have been accommodated by pores 'stretching'. Also, some water may have escaped during freezing so that the pores were not completely filled prior to starting the measurements. However, the validity of these suggestions cannot be

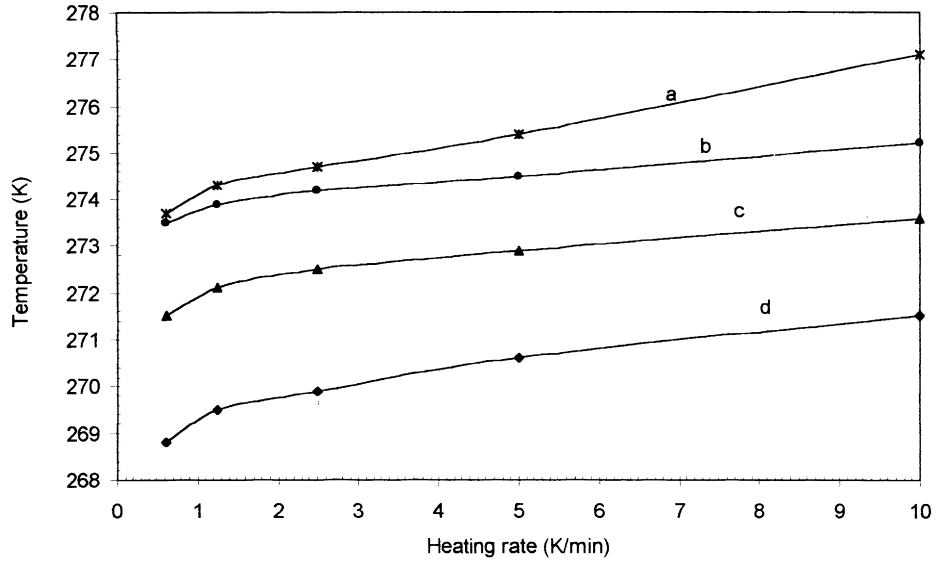

Fig. 7. Effect of thermal lag at different heating rates: (a) represents end of bulk water melting endotherm; (b) represents peak of bulk water melting endotherm; (c) represents heat flow minimum; and (d) represents peak of pore water melting endotherm.

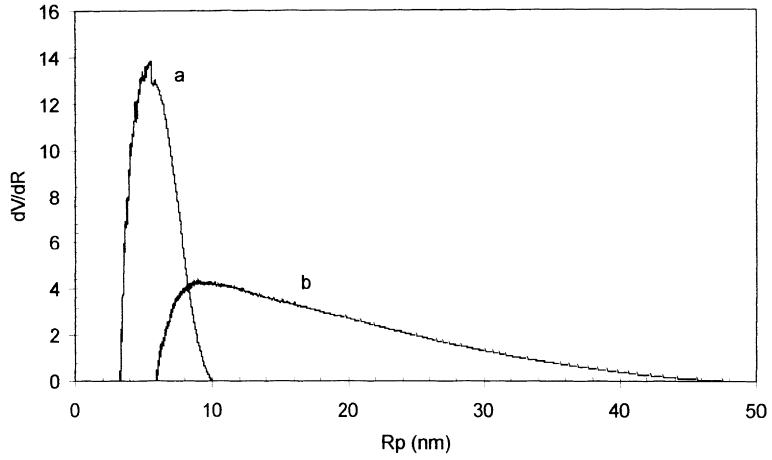

Fig. 8. Comparison of pore size distribution measurements for cellophane; measurements made during heating (curve a) and cooling (curve b).

assessed from the present results and may become the subject for further investigations.

In a separate experiment, a heating run was interrupted part way through the low temperature peak at 267.5 K. This caused a displacement of the first melting peak to higher temperature in the subsequent re-measurement, as demonstrated in Fig. 6. Again, water migration seems to have occurred, but in this case re-freezing appeared to produce larger ice crystals within pores rather than an increase in bulk ice at the surface. The observed change in peak temperature (from 268.7 to 270.1 K) corresponded to an increase of apparent pore radius (based on Eq. (1)) from 8.0 to 11.3 nm. Again, this may demonstrate the elasticity of cellophane, or incomplete filling of pores at the start of the measurements, allowing for an increase in crystal size.

Since the relative peak areas changed with heating rate, slow heating could not be used to avoid thermal lag during thermoporometric measurements. Instead, a small sample size and a temperature correction were preferred. It was observed that thermal lag caused a temperature offset in the heat flow plots which was approximately constant across the measurement temperature range (Fig. 7). Hence, a reasonably accurate melting temperature depression could be obtained by measuring from the end of the bulk water melting peak. Using this temperature correction, pore size distributions, calculated from heat flow measurements made in heating and cooling are compared in Fig. 8.

The measurements made on heating suggested a fairly narrow pore size distribution in cellophane, with a peak at a radius of around 6 nm. In contrast, the measurements made on cooling suggested a much broader distribution containing larger pores and a maximum at a radius of about 10 nm. Most of the pore size distribution indicated by measurements made on heating appeared to be missing from the cooling result and vice versa. Our interpretation of these differences is again based on the migration of water. In the case of measurements during heating, the water melted in the smallest pores, diffused out and re-froze in larger pores or as part of the bulk water. The heat given out by the re-freezing then obscured water melting in larger pores. In contrast, when measurements were made on cooling, as water froze in the larger pores first it was allowed to migrate out the smallest pores, which were consequently not detected.

Alternative explanations may be proposed based on supercooling or slow nucleation in smaller pores, but these do not appear to fit the observations so well. Firstly, as thermoporometry measurements made during cooling detected water in large pores before small pores, any delay in water freezing should cause an apparent shift to smaller pore size, whereas the opposite was observed. Secondly, Ishikiriyama et al. [6] reported good agreement between pore size measurements by a nitrogen gas adsorption–desorption method and thermoporometry measurements during both heating and cooling, for water in a range of polymer membranes. These observations demonstrated that the supercooling of water was not a constraint in detecting pores comparable to or smaller than those observed here in cellophane. Further, it has been suggested that hydrophilic polymers, such as cellulose, may act as heterogeneous nucleation catalysts for ice formation [11].

After completing the DSC measurements, the samples were dried to determine the amounts of water and cellulose. The water determined gravimetrically consistently exceeded that from the DSC measurements, by about 0.5 ± 0.2 g water g^{-1} cellulose. This result agreed better with the quantity of non-freezing water reported by Hatakeyama et al. [36] (about 0.4 g g^{-1}) than that reported by Higuchi et al. [43] (1.06 g g^{-1}). However, it is not clear whether the differences between these results reflect structural differences between the samples studied or errors caused by problems in the measurement method.

6. Discussion

The presence of so-called ‘bound water’ which does not

freeze within cellulose is widely accepted [29,33–43,46]. Although cellulose does not dissolve in water, it does interact strongly and the non-freezing component is believed to represent a layer one or two molecules thick, hydrogen-bonded to cellulose. Similar behaviour has been observed with water absorbed in other polymers [7,44,45,47–49]. Indeed, bound solvent which does not freeze is accounted for in the thermoporometry method established by Brun et al. [1].

In contrast, interpretation of the low temperature melting peak has remained open to debate. Following suggestions which appear to have been made first by Taniguchi and Horigone [44], Hatakeyama et al. [33–38] and others [39–43] have ascribed the low temperature melting peak to water 'weakly interacting' with cellulose, but without presenting any detailed description. By analogy with the non-freezing water, adjacent layers of water molecules might experience 'second-hand' the effects of the polymer surface, particularly hydrogen bonding to hydroxyl groups, placing constraints on molecular motion and packing. However, it is not clear, how such an interaction could explain the changes in the DSC measurements, which were observed following partial melting of samples in the present work. In particular, diffusion of some water out of the cellulose to form bulk ice might be expected to increase the interaction between cellulose and the remaining absorbed water, hence lowering its melting temperature; whereas, the converse occurred. In contrast, melting point depression based on the Gibbs–Thomson effect for water in pores can easily explain these observations. As water was melted in the smallest pores first, it migrated to larger pores or the surface. Here, the water re-froze, since ice was still the thermodynamically preferred state. In these larger crystals, the melting point was higher because the surface to volume ratio was lower.

The nature of water absorbed by polymers has been the subject of several investigations, which generally favoured an explanation of melting point depression based on the Gibbs–Thomson effect. Burghoff and Pusch [45] reported a relatively high heat capacity for water exhibiting a lowered melting point in cellulose acetate membranes, suggesting molecular motion comparable to that of bulk water, rather than constrained like bound water. Similar results were also reported by Ishikiriyama and Todoki [47] for water in poly(methylmethacrylate) hydrogel membranes. Using ^{1}H NMR, Yamada-Nosaka et al. [48] showed that the 'intermediate' water was about 1000 times more mobile than the bound water in methacrylate gels, while the latter still gave a liquid spectrum. Although exchange between 'intermediate' and free water in poly(hydroxyethylmethacrylate) appeared to be relatively slow on the NMR timescale [48], Matsamura et al. [49] reported relatively fast exchange between bound and free water in cellulose acetate.

Melting point depressions have also been observed for water and other liquids in a wide range of polymers and porous solids [1–15,20,21,44,45,47–53]—including combinations where interactions between the porous solid and penetrant liquid are much weaker than between cellulose and water. Jackson and McKenna [53] observed melting point depressions of up to about 36 K for various hydrocarbons in porous glass. Clearly, since only dispersion forces could be operating between the glass and these penetrant liquids, the Gibbs–Thomson effect would appear to offer the best explanation for the melting point depressions observed.

The migration of water out of pores appeared to be a constant feature of DSC measurements on cellophane saturated with water. This is consistent with earlier results presented by Higuchi et al. [43]. The migration of water out of gels during freezing has been discussed in detail by Scherer [50]. Indeed, the migration of benzene and water out of swollen polymer gels during freezing was reported in 1955 by Kuhn et al. [20,21]. Since this effect appears to be caused by mobile penetrant liquid in pores, at temperatures below the 'normal' melting point, possibly in combination with crystals of the frozen penetrant (e.g. in larger pores or at the surface), it might be expected frequently—if not always—during thermoporometry. However, we believe this is the first time there has been any attempt to quantify the rate of water migration out of the sample and to discuss the effect in terms of sample structure and other diffusion measurements.

The cross-section structure of cellophane has been investigated by several authors using a variety of techniques [54–61]. The results of these investigations are not entirely conclusive and have been interpreted in different ways. From our interpretation of the published data, augmented with some (presently unreported) studies of our own, it appears that cellophane has a differentiated layer structure, with a porous central core sandwiched between relatively dense surface 'skin' layers up to about 1 μm thick. It seems likely that the postulated movement of water during the DSC measurements took place from the porous core through the 'skin' and re-freezing occurred as water from pores contacted ice crystals at the surface.

Our data showed that water moved from the pores to the bulk ice crystals according to the Eqs. (4a) and (4b), for the sample described in Table 2. The pre-exponential factor represents the quantity (in milligrams) of water available to migrate. The constant 0.18, in Eq. (4b), suggests that this amount of bulk water (also in milligrams) existed at the surface, prior to water migration from pores. The rate of water migration can be obtained by differentiating Eq. (4a):

$$\text{Rate of migration}: \frac{\mathrm{d}Q_{\mathrm{p}}}{\mathrm{d}t} = \frac{-0.65}{550} \exp\{-t/550\} \qquad (5)$$

At time $t = 0$, this gave a rate of migration of -1.2×10^{-6} g s^{-1} (the negative sign indicating movement away from the pores), for the sample described in Table 2. Assuming diffusion through a dense skin region 1 μm thick to be

the rate determining factor, fitting the results obtained to Fick's first law of diffusion:

$$\frac{dQ}{dt} = -DA\frac{dc}{dx} \quad (6)$$

where A is area through which diffusion took place and dc/dx is concentration gradient, gave a value of about 1×10^{-13} m^2 s^{-1} for the diffusion coefficient, D.

This is too small, by a factor of 10^3, for the diffusion coefficient of water in highly swollen cellophane. Yasuda et al. [62] reported a value of 3.2×10^{-10} m^2 s^{-1} for water in swollen cellophane; Brown and Chitumbo [63] also obtained a value of 4.1×10^{-10} m^2 s^{-1} for water in swollen cross-linked cellulose gel. Our own (presently unreported) measurements using FTIR-ATR and field gradient NMR spectroscopy gave values of 5.6×10^{-10} and 9×10^{-10} m^2 s^{-1}, respectively for the diffusion coefficient, with the differences being attributable to the cellophane skin–core structure.

However, it seems likely that the cellophane 'skin' may not have been in a highly swollen state during the DSC experiments. Instead, water may have drained out of the 'skin' as ice formed at the surface and in pores in the core during the initial freezing step. This process would be assisted if the freezing point of water was strongly depressed in the surface layer, either because of the very small size of pores or through direct interaction with cellulose chains. In fact, this effect was observed by comparing pore size distributions measured on heating and cooling (Fig. 7).

The migration of water during DSC experiments probably took place through freeze-dried cellulose. The diffusion coefficient for water in cellulose at relatively low levels of hydration (up to 0.45 g g^{-1} water in cellulose) has been measured by several authors. Ebrahimzadeh and McQueen [64] reported values between about 3×10^{-14} and 3×10^{-13} m^2 s^{-1}, for cellophane film containing plasticiser; Kawaguchi et al. [65] found diffusivity increased from about 2×10^{-15} up to 8×10^{-13} m^2 s^{-1} for partially cross-linked cellophane over a range of moisture levels. In the earliest work, Newns [66] reported diffusion coefficients ranging from 1×10^{-14} up to about 2×10^{-12} m^2 s^{-1} for saponified cellulose acetate film. These values are more consistent with the diffusion coefficient measured in the present work.

Regarding pore size measurements, it is clear that thermoporometry results must be viewed with caution. The peak in the pore volume distribution for water swollen cellophane at a radius of about 6 nm, indicated from measurements during heating, and the tail in the distribution extending towards 50 nm radius, indicated from results during cooling, may both have been real. However, changes in shapes observed for the heat flow vs. temperature plots at different heating rates and a comparison of the pore size distributions from heating and cooling measurements demonstrated that the results were significantly affected by measurement conditions. As such, they cannot be regarded as absolutely correct.

7. Conclusions

The observation by DSC of a low temperature water melting peak in wet cellophane was due to the Gibbs–Thomson effect. This is consistent with the interpretation given by Burghoff and Pusch [45] and others [47–49] for low temperature water melting peak observed in cellulose acetate and other polymers.

A pore size distribution with radii between about 5 and 50 nm was indicated for water-swollen cellophane. However, the exact distribution could not be determined with any confidence, since the results changed dramatically with experimental conditions.

While the Gibbs–Thomson effect gives a relationship between crystal size and melting point, there can be problems in using melting point depression to measure pore size distributions (thermoporometry). In the present work, migration and re-freezing of melted pore water affected the shape of the heat flow-temperature plot during DSC measurements made on heating. Similar results were reported by Higuchi for water in cellophane [43] and by several other authors for various combinations of porous substrate and penetrant liquid [20,21,50]. Migration prior to freezing also affected the shape of the heat flow-temperature plot for DSC measurements made on cooling. In either case, parts of the pore size distribution were missing from the calculated results.

There is no reason why the migration should only occur during measurements. Indeed, it seems likely that migration occurred during the preliminary freezing step, prior to making any measurements, causing the cellophane 'skin' to dry out.

The water migration observed during the DSC measurements was consistent with a diffusion process through a surface layer of relatively dry cellulose about 1 μm thick, which separated the porous cellophane core from bulk water at the surface.

References

[1] Brun M, Lallemand A, Quinson J-F, Eyraud C. Thermochim Acta 1977;21:59–88.
[2] Quinson JF, Dumas J, Serughetti J. J Non-cryst Solids 1986;79:397–404.
[3] Nakao S-I. J Membr Sci 1994;96(1/2):131–65.
[4] Kim KJ, Fane AG, Aim RB, Liu MG, Jonsson G, Tessaro IC, Broek AP, Bargeman D. J Membr Sci 1994;87(1/2):35–46.
[5] Escribano S, Aldebert P, Pineri M. Electrochim Acta 1998;43-(14/15):2195–202.
[6] Ishikiriyama K, Sakamoto A, Todoki M, Tayama T, Tanaka K, Kobayashi T. Thermochim Acta 1995;267:169–80.
[7] Price DM, Bashir Z. Thermochim Acta 1995;249:351–66.
[8] Madkour T, Mark JE. Polym Bull 1993;31(5):615–21.

[9] Broek AP, Bargeman D, Sprengers ED, Smolders CA. Int J Artificial Organs 1992;15(1):25–8.
[10] Broek AP, Teunis HA, Bargeman D, Sprengers ED, Smolders CA. J Membr Sci 1992;73:143–52.
[11] Cuperus FP, Bargeman D, Smolders CA. J Membr Sci 1992;66:45–53.
[12] Quinson JF, Mameri N, Guihard L, Bariou B. J Membr Sci 1991;58(2):191–200.
[13] Tammann G. Z Anorg Allg Chem 1920;110:166–8 Chemical Abstracts 1920; 14:3553.
[14] Meissner F. Z Anorg Allg Chem 1920;110:169–86 Chemical Abstracts 1920; 14:3553.
[15] Kubelka P. Z Elektrochem 1932;38:611–4 Chemical Abstracts 1932; 26:5241.
[16] Reiss H, Wilson IB. J Colloid Sci 1948;3:551–61.
[17] Still RC, Skapski AS. J Chem Phys 1956;24(4):644–51.
[18] Woodruff DP. The solid–liquid interface, Cambridge solid state science series, Cambridge: Cambridge University Press, 1973.
[19] Skapski AS. J Chem Phys 1959;31:573.
[20] Kuhn W, Majer H. Z Phys Chem (Frankfurt) 1955;3:330–40.
[21] Kuhn W, Peterli E, Majer H. J Polym Sci 1955;16:539–48.
[22] Barrett EP, Joyner LG, Halenda PP. J Am Chem Soc 1951;73:373–80.
[23] Morita Z, Ishida H, Shimamoto H. J Membr Sci 1989;46:283–98.
[24] Kuga S. J. Colloid Interface Sci 1980;77(2):413–7.
[25] Stratton RA. J Polym Sci: Polym Chem Ed 1973;11:535–44.
[26] Bradley SA, Carr SH. J Polym Sci: Polym Phys Ed 1976;14:111–24.
[27] Baum GA. J Appl Polym Sci 1973;17:2855–66.
[28] Hongo T, Koizumi T, Yamane C, Okajima K. Polym J 1996;28(12):1077–83.
[29] Yano S, Hatakeyama H. Polymer 1988;29:566–70.
[30] Hermans RH, Weidinger AJ. J Colloid Sci 1946;1:185–93.
[31] Sakurada I, Fuchino K. Riken-Iho (Bull Inst Phys Chem Res) 1935;14:171.
[32] Sakurada I, Fuchino K. Riken-Iho (Bull Inst Phys Chem Res) 1936;15:973.
[33] Hatakeyama H, Hatakeyama T. Thermochim Acta 1998;308(1/2):3–22.
[34] Yoshida H, Hatakeyama H, Hatakeyama T. J Therm Anal 1993;40(2):483–9.
[35] Yoshida H, Hatakeyama T, Hatakeyama H. In: Glasser W, Hatakeyama H, editors. Viscoelasticity of biomaterials, ACS Symp Ser, 489. Washington, DC: American Chemical Society, 1992. pp. 217–30.
[36] Hatakeyama T, Nakamura K, Hatakeyama H. In: Kennedy JF, Phillips GO, Williams PA, editors. Cellulose sources and exploitation: industrial utilization, biotechnology and physico-chemical properties, Chichester, UK: Ellis Horwood, 1990 see chap. 2, 13–9.
[37] Hatakeyama T, Hatakeyama H. In: Kennedy JF, Phillips GO, Wedlock DJ, Williams PA, editors. Cellulose and its derivatives: chemistry, biochemistry and applications, Chichester, UK: Ellis Horwood, 1985 see chap. 7, 87–94.
[38] Nakamura K, Hatakeyama T, Hatakeyama H. Text Res J 1981;51(9):607–13.
[39] Weise U, Maloney T, Paulapuro H. Cellulose 1996;3:189–202.
[40] Yamauchi T, Murakami K. J Pulp Paper Sci 1991;17(6):J223–6.
[41] Bertran MS, Dale BE. J Appl Polym Sci 1986;32(3):4241–53.
[42] Kruglitsky NN, Polishchuk TN, Privalko VP, Vyazmitina OM. Ukr Khim Zh 1985;51(12):1250–4.
[43] Higuchi A, Komiyama J, Iijima T. Polym Bull 1984;11:203–8.
[44] Taniguchi Y, Horigome S. J Appl Polym Sci 1975;19:2743–8.
[45] Burhoff HG, Pusch W. J Appl Polym Sci 1979;23:473.
[46] Nielson OF, Lindstrom T, Lund PA. Acta Chem Scand 1982;A36(7):623–5.
[47] Ishikiriyama K, Todoki M. J Polym Sci: Part B Polym Phys 1995;33:791–800.
[48] Yamada-Nosaka A, Ishikiriyama M, Todoki M, Tanzawa H. J Appl Polym Sci 1990;39:2443–52.
[49] Matsumura K, Hayamizu K, Nakane T, Yanagishita H, Yamamoto O. J Polym Sci: Part B Polym Phys 1987;25:2149–63.
[50] Scherer GW. J Non-cryst Solids 1993;155:1–25.
[51] van Miltenburg JC, van der Eerden JP. J Cryst Growth 1993;128:1143–9.
[52] Handa YP, Zakrzewski M, Fairbridge C. J Phys Chem 1992;96:8594–9.
[53] Jackson CL, McKenna GB. J Chem Phys 1990;93(12):9002–11.
[54] Fink H-P, Purz HJ, Weigel P. Das Papier 1997;51(12):643–52.
[55] Irklei VM, Ochkivskii AP, Ryabchenko AS, Nosov NP. Vysokomol Soedin Ser B 1972;14(9):709–11 Chemical Abstracts 1973; 78:45277x.
[56] Jayme G, Balser K. Das Papier 1967;21(10A):678–88.
[57] Jayme G, Balser K. Das Papier 1965;19(10A):741–9.
[58] Jayme G, Balser K. Ind Chim Belge 1967;32:365–72.
[59] Philipp B, Baudisch J, Bohlmann A. Faserforsch und Textiltech 1967;18(11):511–7.
[60] Hilyard NC. J Appl Polym Sci 1967;11:1315–23.
[61] Pearse HA, Priest DJ, Schimmell RJ, White AG. Tappi 1963;46:622.
[62] Yasuda H, Lamaze CE, Peterlin A. J Polym Sci: Part A-2 1971;9:1117–31.
[63] Brown W, Chitumbo K. JCS Trans Faraday Soc 1 1975;71:1–11.
[64] Ebrahimzadeh PR, McQueen DH. J Mater Sci 1998;33:1201–9.
[65] Kawaguchi M, Taniguchi T, Tochigi K, Takizawa A. J Appl Polym Sci 1975;19:2515–27.
[66] Newns AC. Trans Faraday Soc 1956;52:1533–45.